ISSN: 2688-8645

Design of Intelligent Foam Drainage Equipment with UAV Automatic Agent Replenishment for Low-Pressure Gas Wells: An Electromechanical System

Boya Wu, Benjie Li and Yiqin Xiong

School of Mechanical and Electrical Engineering, Southwest Petroleum University, Chengdu Sichuan, 610000, China

Abstract

In the mid-to-late production stages of low-pressure gas wells, wellbore liquid loading becomes a prominent issue. Traditional manual foam drainage agent injection suffers from inaccuracies in timing, agent waste, and high labor intensity. This paper presents the design of an intelligent foam drainage system integrated with UAV-based automatic agent replenishment, achieving core functions such as automatic precise injection, closed-loop control of concentration and flow rate, remote monitoring, and unmanned UAV agent replenishment. The equipment adopts a skid-mounted integrated structure and features an innovatively designed purely mechanical passive UAV-to-equipment liquid docking module. The electrical control system is centered on the STM32F103C8T6 microcontroller and incorporates the FreeRTOS real-time operating system to enable multitasking scheduling. The injection control employs a PID algorithm, with a first-order system model established that accounts for wellhead pressure disturbances; simulation results verify its fast response and strong disturbance rejection capability. Cloud-edge communication is implemented using the MQTT protocol to connect to the Alibaba Cloud IoT platform, enabling real-time data uploading and remote command issuance. Results demonstrate that this design significantly improves foam drainage efficiency, reduces agent consumption and labor costs, and is well-suited for long-term unattended operation in remote gas wells.

Keywords

Intelligent Foam Drainage Equipment; UAV Automatic Agent Replenishment; Mechatronics Integration; PID Closed-loop Control; FreeRTOS; Cloud-edge Communication.

1. Introduction

As low-pressure gas wells enter the mid-to-late production stages, wellbore liquid loading becomes increasingly severe, resulting in a substantial decline in gas production rate or even complete shut-in. Foam drainage gas recovery technology involves injecting a foaming agent into the wellbore to generate low-density foam at the bottomhole, which carries the accumulated liquids to the surface[1]. This method offers the advantages of cost-effectiveness and strong adaptability. However, conventional manual injection approaches suffer from several shortcomings, including imprecise timing of injection, significant foaming agent waste, high labor intensity, and elevated safety risks associated with high-altitude operations[2,3]. These limitations make it difficult to meet the requirements for long-term unattended operation in low-pressure gas wells.

To address the above challenges, this paper proposes an intelligent foam drainage equipment integrated with unmanned aerial vehicle (UAV) automatic foaming agent replenishment. The core functions of the equipment include:

ISSN: 2688-8645

(1) Automatic precise injection function: real-time assessment of liquid loading status based on gas well production parameters, with automatic adjustment of foaming agent injection volume and frequency;

(2) Closed-loop concentration/flow control function: dynamic adjustment of pump speed or valve opening through sensor feedback and PID algorithm to maintain stable foaming agent concentration;

(3) Remote monitoring and communication function: real-time data uploading to a cloud platform for fault diagnosis and parameter optimization;

(4) UAV automatic replenishment function: integration of a dedicated docking interface to support precise UAV landing and agent injection;

(5) Environmental adaptability and safety features: explosion-proof, corrosion-resistant, and low-power design.

Referring to domestic commercial foam drainage devices and relevant process standards, combined with innovative requirements, the main technical specifications are established as follows: pressure rating ≥ 15 MPa, daily injection volume adjustable from 0 to 500 L, injection accuracy ±5%, foaming agent storage capacity ≥ 20 L, operating temperature range −20°C to 60°C, power supply via solar + lithium battery, communication support for WiFi/4G and MQTT protocol, liquid loading diagnosis accuracy ≥ 95%, system response time ≤ 5 min, and explosion-proof rating Ex d IIB T6.

Based on the above requirements, this paper optimizes the conventional foam drainage equipment by developing an integrated electromechanical system that encompasses storage, preparation, and injection modules. This achieves full-process automation from agent storage and automatic dilution to precise injection, providing a novel approach for efficient liquid unloading in low-pressure gas wells.

2. Scheme Design

2.1. Overall Structure and Skid-Mounted Integrated Layout

The intelligent foam drainage equipment adopts a skid-mounted integrated design, featuring an overall rectangular enclosure structure that facilitates hoisting, transportation, and rapid deployment at the wellsite. The enclosure is fabricated by welding steel plates and treated with anti-corrosion spray coating on the surface to withstand harsh outdoor environments characterized by high humidity, salt spray, and large temperature variations.

The top of the equipment is designed as a flat aluminum alloy large platform with a diameter of 1000 mm (thickness 5 mm). The platform surface is covered with a 3 mm thick rubber buffer pad to absorb the impact of UAV landing. Two circular liquid replenishment docking interfaces are arranged on the platform, each equipped with a conical guide funnel and buffer structure, capable of tolerating up to ±10 cm horizontal positioning deviation of the UAV, thereby ensuring precise docking.

The internal layout follows a modular design, mainly comprising:

Left side: Large water storage tank (used for preparation water of the foaming agent);

Middle: Side-by-side green foaming agent stock tank and red defoaming agent stock tank (each with capacity meeting the ≥20 L design requirement and supporting UAV replenishment expansion);

Right side: Pump group system (multiple independent pumps, enabling differentiated injection strategies for different wellheads);

Front: Control cabinet (integrating the human-machine interface, electrical interfaces, and STM32 core board).

ISSN: 2688-8645

The piping system employs color coding (blue for water line, green for foaming agent line, red for defoaming agent line) to facilitate on-site maintenance and troubleshooting. The overall dimensions and weight distribution have been optimized to ensure a stable center of gravity, allowing direct fixation onto a wellsite concrete foundation or skid base for use.

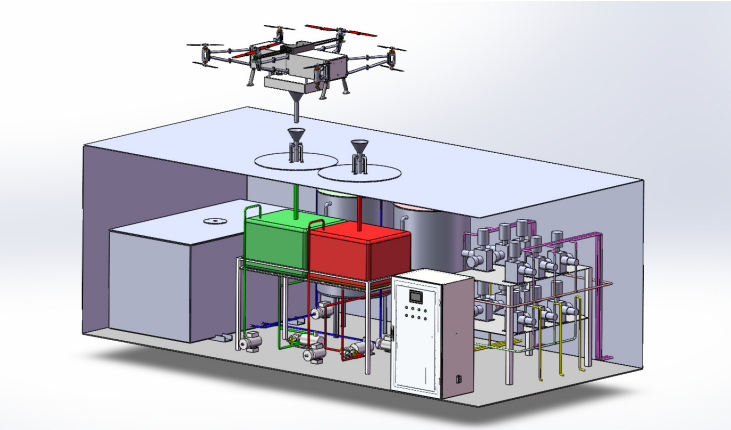

Figure 1. Overall Appearance of the Intelligent Foam Drainage Equipment

2.2. UAV Automatic Liquid Replenishment Module Design

The UAV automatic liquid replenishment module is the most significant innovation in this design. Installed on the top of the equipment, it adopts a purely mechanical passive triggering scheme that requires no electrical power drive or active control. This provides notable advantages, including structural simplicity, high reliability, and strong resistance to harsh environmental conditions[4].

The module comprises two main components: the ground-fixed replenishment interface and the UAV-side 30 L agent tank docking mechanism.

The ground-fixed replenishment interface includes:

(1) A circular platform (diameter 1000 mm, aluminum alloy, with rubber buffer pad on the surface);
(2) A conical funnel (upper diameter 250 mm, lower diameter 50 mm, depth 180 mm, cone angle 45°, stainless steel material, wall thickness 5 mm);
(3) A cross-shaped support bracket at the funnel bottom + a centrally fixed ejector pin (used to trigger the agent tank valve).

The UAV agent tank is constructed from corrosion-resistant PP plastic, with dimensions of 650 mm (length) × 450 mm (width) × 120 mm (height) and a capacity of 30 L. The tank weighs approximately 32 kg empty and about 80 kg when fully loaded, satisfying the payload requirements of large quadrotor UAVs. The tank bottom incorporates a slight slope converging toward the center to ensure complete agent drainage. A conical probe is integrated at the center (total length 150 mm, upper diameter 100 mm, lower outer diameter 50 mm, internal channel diameter 40 mm).

The probe incorporates a spring-loaded plunger-type passive valve internally: under normal conditions, the spring pushes the valve core downward to seal the lower end. When the probe is fully inserted into the funnel, the fixed ejector pin from below pushes the valve core upward by approximately 15 mm, compressing the spring and opening an annular gap along with the lower end opening, thereby forming a large-flow discharge channel. Upon completion of replenishment, the UAV takes off, withdrawing the probe, and the spring immediately resets to close the valve, achieving zero-drip separation.

The entire working process relies solely on gravity and mechanical guidance: the UAV performs coarse positioning and descends → the conical surface of the probe automatically centers → the

ISSN: 2688-8645

landing gear buffers touchdown → the probe inserts and triggers the valve → gravity-driven discharge occurs → automatic separation upon takeoff.

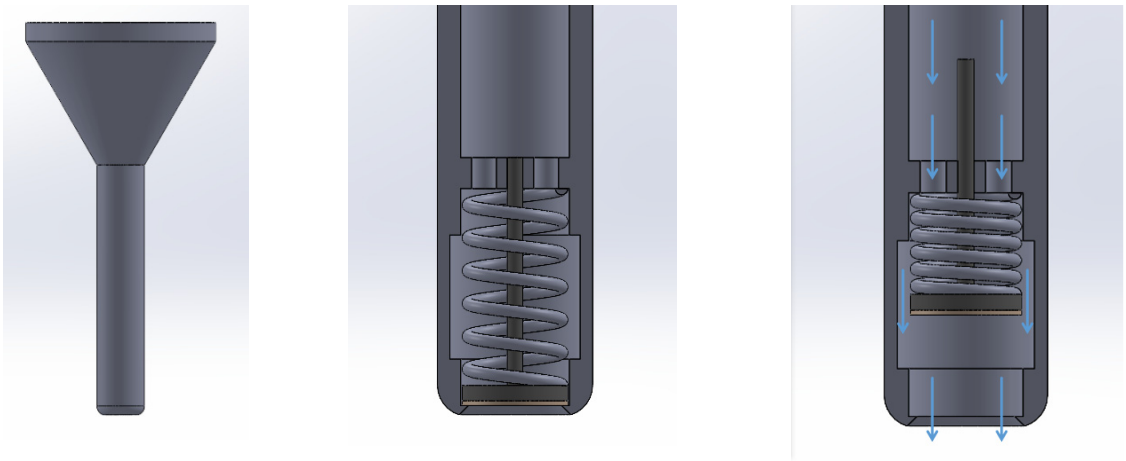

Figure 2. Cross-Sectional View of the Probe and Passive Valve

2.3. Strength Check of the UAV Refilling Module

To ensure the structural safety of the UAV automatic refilling module during the actual docking process, strength checks were performed on the key loaded components. In the actual landing scenario, the UAV carries a 30 L chemical tank with a total mass of 80 kg and approaches the platform at a low speed of 0.4 m/s. The probe tip first contacts the inner wall of the funnel, and gradual deceleration and centering are achieved through frictional and component forces generated by the conical contact surface. Only when the probe is aligned and approaches the bottom ejector pin do the landing legs contact the platform. Therefore, the thinnest lower part of the probe mainly bears axial compressive load and bending load induced by lateral guiding, requiring combined stress verification.

Calculation of axial docking load The process is simplified as a progressive buffered collision, and the maximum axial force is estimated using the principle of conservation of mechanical energy:

$$F_{\max} = \frac{mv^2}{2\delta} + \mu mg\frac{L}{\delta} \tag{1}$$

where

m = total mass = 80 kg

v = landing velocity = 0.4 m/s

δ = buffer distance ≈ 0.02 m

μ = friction coefficient ≈ 0.3

L = guiding path length ≈ 0.15 m

The calculation yields a maximum axial force of approximately 3200 N, which satisfies the design safety margin.

Bending moment due to lateral guiding force The lateral guiding component force at the probe root is conservatively taken as 50% of the axial force (1600 N), producing a bending moment:

$$M = F_{\text{lateral}} \times l \tag{2}$$

ISSN: 2688-8645

The maximum bending stress is calculated using the beam bending formula from strength of materials:

$$\sigma_b = \frac{M}{W} \approx 30.7\,\text{MPa} \tag{3}$$

where W is the section modulus of the probe cross-section

The axial compressive stress is:

$$\sigma_c = \frac{F_{\max}}{A} \approx 28.5\,\text{MPa} \tag{4}$$

Combined stress check using the third strength theory Using the maximum shear stress theory (third strength theory), the principal stress difference is approximately 59.2 MPa, which is significantly lower than the allowable stress of the selected stainless steel material (137 MPa), providing ample safety margin. Similar checks were performed on the lower part of the conical funnel, and the results also meet the requirements.

The strength verification confirms that the UAV refilling module maintains sufficient structural safety and reliability under the designed docking conditions, even considering conservative load assumptions and potential misalignment during landing.

This completes the strength analysis of the innovative passive mechanical refilling interface, laying a solid foundation for the practical engineering application of the UAV-assisted refilling function.

3. Control Design

3.1. Embedded Software Architecture and FreeRTOS Multi-Task Implementation

To meet the real-time concurrent requirements of the intelligent foam drainage equipment for high-frequency sensor data acquisition, closed-loop control, cloud communication, and fault diagnosis, this paper abandons the traditional bare-metal foreground-background polling approach and adopts FreeRTOS V10.4.3 real-time operating system to construct the embedded software architecture. FreeRTOS is highly suitable for the resource-constrained STM32F103C8T6 platform (64 KB Flash, 20 KB SRAM) due to its small kernel footprint (approximately 12 KB Flash usage), mature preemptive scheduling, and strong portability.

The software employs a typical three-layer modular structure:

(1) Low-level driver layer: Encapsulates peripheral drivers such as ADC, TIM, USART, and GPIO based on the STM32 standard peripheral library;

(2) Operating system layer: FreeRTOS kernel, providing task management, message queues, semaphores, mutexes, and timer services;

(3) Application task layer: Divided into four core tasks, ordered by priority from high to low as follows:

1) Data acquisition and local display task (highest priority, ensuring real-time sensor data);

2) Foaming agent injection control task (core control task);

3) Communication task (MQTT cloud interaction);

4) System monitoring task (lowest priority, responsible for watchdog feeding, abnormal logging.

Inter-task communication primarily relies on FreeRTOS message queues (for transferring sensor data and control commands) and semaphores/mutexes (to protect shared global variables such as the xSensorData structure). To further optimize resource usage, all task stacks are statically allocated to avoid fragmentation risks associated with dynamic allocation. The

ISSN: 2688-8645

idle task hook function implements a low-power STOP mode, which, combined with solar + lithium battery power supply, significantly extends field endurance.

Upon system power-up, peripheral initialization is first completed (including ADC multi-channel DMA, TIM PWM, USART communication with ESP8266, etc.), followed by creation of message queues, semaphores, mutexes, and task stacks. Finally, the scheduler is started to enter the multi-task running state. Actual testing shows that, compared to the bare-metal scheme, FreeRTOS's preemptive scheduling reduces the response latency of the highest-priority task (data acquisition) from tens of milliseconds to less than 5 ms, with average CPU load controlled below 35%, fully satisfying the on-site gas well system response time requirement of ≤5 min.

The data acquisition and local display task adopts an event-driven mechanism, refreshing the OLED screen only upon ADC sampling completion or significant data changes, thereby reducing power consumption. Meanwhile, the UploadHeight function prepares foam height data for inclusion in the upload queue, providing a foundation for subsequent cloud-based analysis. This task features a clear process and strong real-time performance, serving as the cornerstone for reliable operation of the entire control system.

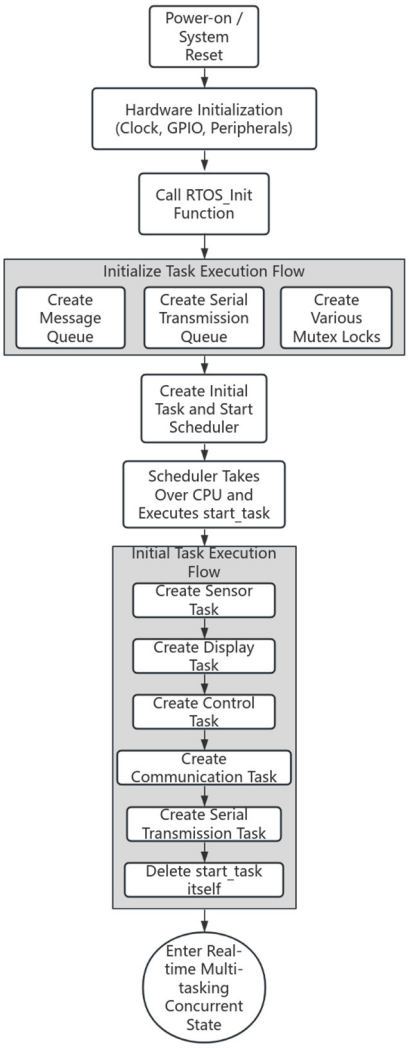

Figure 3. Task Initialization and Creation Flowchart

3.2. PID Closed-Loop Control Algorithm for Foaming Agent Injection

The foaming agent injection control task is the most critical functional module of the entire system. It determines the injection volume based on real-time foam height (or predicted liquid loading status) and precisely drives the variable-frequency pump in a closed-loop manner to

ISSN: 2688-8645

inject the agent into the wellbore or wellhead. In actual operating conditions of low-pressure gas wells, severe fluctuations in wellhead pressure (typically 0.1–1.0 MPa), changes in pipeline resistance, and temperature-dependent variations in agent viscosity can all cause significant deviations in open-loop timed injection[5]. Excessive concentration leads to agent waste, while insufficient concentration results in poor liquid unloading performance. Therefore, closed-loop control is essential to enable the actual injection flow rate to rapidly and stably track the target value.

This paper selects the classic PID control algorithm as the core control law. With its simple structure, clear physical meaning of parameters, and strong robustness, it is highly suitable for injection scenarios characterized by large pressure disturbances but requiring explicit steady-state accuracy and response speed. The continuous form of the PID controller is:

$$u(t) = K_p e(t) + K_i \int_0^t e(\tau)\, d\tau + K_d \frac{de(t)}{dt} \tag{5}$$

$$e(t) = Q_{\text{set}} - Q_{\text{act}} \tag{6}$$

where

$e(t)$ is the flow deviation (difference between target flow rate and actual flow rate);

K_p is the proportional gain, determining response speed;

K_i is the integral gain, eliminating steady-state error;

K_d is the derivative gain, suppressing overshoot and oscillations.

Considering the implementation on the STM32 digital controller, this paper adopts the positional PID algorithm (rather than the incremental form). Its discrete form is:

$$u(k) = K_p e(k) + K_i \sum_{i=0}^{k} e(i) \cdot T + K_d \frac{e(k) - e(k-1)}{T} \tag{7}$$

The positional algorithm facilitates direct application of upper and lower limits to the control output (PWM duty cycle or pump speed), avoiding integral windup that could cause actuator overshoot or reverse saturation. This is particularly appropriate for practical scenarios where the dosing pump speed has a physical range.

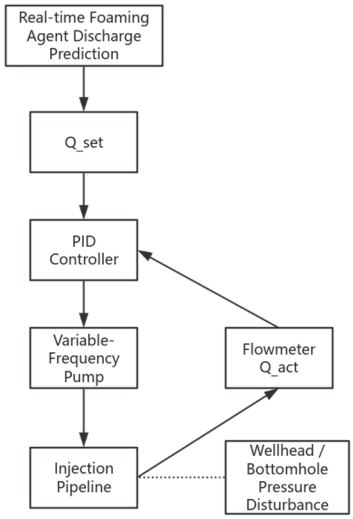

Figure 4. Block Diagram of the Injection Flow Rate Control System

3.3. Modeling and Parameter Tuning of the Injection Flow Rate Control System

To achieve effective application of the PID controller under the complex operating conditions of low-pressure gas wells, it is necessary to establish an accurate mathematical model of the injection flow rate control system and perform parameter tuning accordingly. The system

ISSN: 2688-8645

primarily consists of a variable-frequency pump, pipelines, flowmeter, and controller. Its dynamic characteristics can be approximated as a first-order inertial element, with the transfer function given by:

$$G(s) = \frac{K}{\tau s + 1} \tag{8}$$

where:

K is the system static gain

τ is the time constant, reflecting the response time from pump speed change to stabilized flow rate

In actual operating conditions, wellhead pressure disturbance P(t) P(t) P(t) is the primary disturbance source, directly affecting the pump's output flow rate. Considering the influence of disturbances, the system output flow rate can be expressed as:

$$Q(s) = G(s)U(s) + G_d(s)P(s) \tag{9}$$

where $G_d(s)$ is the disturbance transfer function, and the typical range of pressure disturbances is 0.1–1.0 MPa.

The main parameters of the system are summarized in the following table:

Table 1. Main Parameters of the Foaming Agent Injection Flow Rate Control System

Parameter	Symbol	Value	Unit	Description
Target flow setpoint	Q_set	dynamic	L/h	Based on liquid loading prediction or cloud commands
Control system gain	K	1.2	-	Determined by pump characteristics
Time constant	τ	0.8	s	Pump response time
Pressure disturbance range	P	0.1~1.0	MPa	Actual wellhead fluctuations
Flow meter accuracy	-	±0.2	L/min	Real-time feedback accuracy

Based on the above first-order model, the classic Ziegler-Nichols ultimate sensitivity method is employed for preliminary PID parameter tuning. The steps are as follows:

Set $K_i = 0$ and $K_d = 0$, retaining only the proportional term, and gradually increase K_p until the system exhibits sustained equal-amplitude oscillations. Record the critical gain K_u and oscillation period T_u at this point.

According to the Ziegler-Nichols rules, the initial parameters are calculated as:

$$K_p = 0.6K_u \tag{10}$$

$$K_i = \frac{1.2K_u}{T_u} \tag{11}$$

$$K_d = 0.075K_uT_u \tag{12}$$

Considering the severe pressure fluctuations in gas wells and the engineering requirements for fast response with minimal overshoot, the initial parameters are fine-tuned. The final selected values are:

ISSN: 2688-8645

$$K_p = 1.8, \quad K_i = 0.45, \quad K_d = 0.36 \tag{13}$$

This set of parameters demonstrates good overall performance in simulation: fast response, controllable overshoot, and no noticeable steady-state error. In the positional PID algorithm, additional measures such as integral separation, anti-windup protection, and output limiting (PWM duty cycle restricted to 0–100%) are incorporated to further enhance stability and safety during practical execution.

3.4. Simulation Verification and Performance Analysis

To verify the actual control performance of the designed PID controller under wellhead pressure disturbance conditions in low-pressure gas wells, this paper develops a simulation model using Python (based on the numpy, scipy, and matplotlib libraries). Step response and disturbance rejection tests are conducted on the injection flow rate control system, with comparisons made against the uncontrolled open-loop system.

The simulation conditions are set as follows:

(1) Target flow step change: from 0 L/h to a target value of 200 L/h (typical demand for a single medium-to-low production gas well);
(2) System model: first-order inertial element with parameters $K = 1.2$, $\tau = 0.8$;
(3) Pressure disturbance: random disturbance with amplitude ±0.6 MPa superimposed after t = 3 s ;
(4) Sampling period: T = 0.02 s;
(5) PID parameters: $K_p = 1.8$, $K_i = 0.45$, $K_d = 0.36$;
(6) Total simulation duration: 10 s.

The simulation results are shown in Figure 7. From the response curves, it can be observed that:

The open-loop system exhibits severe flow fluctuations under disturbance and fails to stably track the target value;

The PID closed-loop system rises rapidly in the initial phase, reaching near the target value in approximately 1.5 s; after t = 3 s, despite significant pressure disturbance, the controller quickly regulates the flow, limiting fluctuations to a very small range and ultimately achieving stable tracking of the target flow rate, demonstrating excellent disturbance rejection capability.

The main performance indicators are compared in the following table:

Table 2. Performance Comparison between PID Closed-Loop and Open-Loop Systems

Performance Indicator	Open-Loop System	PID Closed-Loop System	Improvement	Performance Indicator
Overshoot	Unstable	7.9%	Significantly reduced	Overshoot
Settling time to ±5% error band	>10 s	2.6 s	Shortened by 74%	Settling time to ±5% error band
Steady-state error	±2.1 L/h	±0.22 L/h	Reduced by 89%	Steady-state error
Disturbance recovery time	—	<1.2 s	—	Disturbance recovery time

The simulation results demonstrate that the designed PID controller achieves fast response (settling time shortened by 74%), low overshoot (7.9%), and extremely small steady-state error (±0.22 L/h, relative error <1.1%) even under large wellhead pressure fluctuations. This fully meets the engineering requirements of system response time ≤5 min and injection accuracy ±5%. The performance improvement significantly enhances foaming agent utilization efficiency and reduces drainage efficiency losses caused by agent overdose or insufficiency.

ISSN: 2688-8645

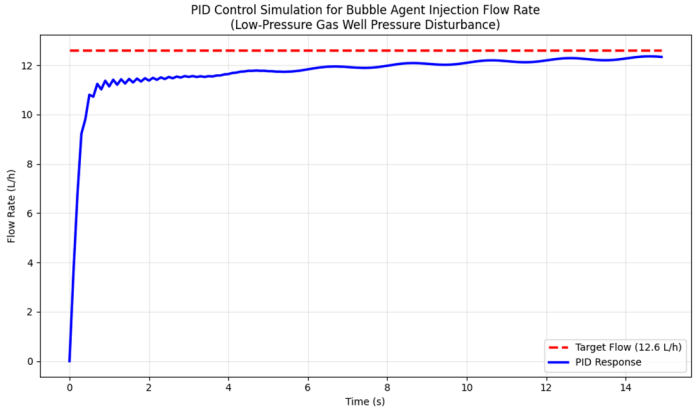

Figure 5. Response Curve of Foaming Agent Injection Flow Rate under PID Control

This section verifies the effectiveness and robustness of the PID controller through simulation, providing a reliable theoretical foundation for subsequent embedded code implementation and field trials.

4. Conclusion

This paper addresses the liquid loading issue in low-pressure gas wells by designing an intelligent foam drainage equipment integrated with UAV automatic foaming agent replenishment. A complete electromechanical integrated solution has been developed, encompassing mechanical structure, electrical control hardware, FreeRTOS-based software, PID closed-loop control, and cloud-edge communication.

The purely mechanical passive liquid replenishment module, along with its strength verification, ensures high reliability. The disturbance rejection performance of the PID controller has been validated through simulation. Overall, the system achieves precise closed-loop injection and unattended long-term operation.

Compared to traditional manual foam drainage operations, this equipment significantly improves injection efficiency, reduces foaming agent consumption and labor costs, and demonstrates broad prospects for engineering applications.

Future work may focus on further optimizing fuzzy PID algorithms and developing multi-UAV collaborative replenishment strategies to enhance the system's level of intelligence.

References

[1] Zhao, S., et al. Research and development of new intelligent foaming agent for foam drainage gas recovery. Petroleum, 2024.

[2] Niu, B. Construction and Application of the Technological Innovation Management System for Foam Drainage in Gas Wells. Atlantis Press, 2025.

[3] Wang, Z. Research and application of intelligent foam drainage control system for gas wells. Oil Production Engineering, 2021.

[4] Xu, Z., et al. Vision Algorithms for UAVs Aerial Refueling Using Probe-and-Drogue Mechanism. Atlantis Press, 2014.

[5] Fang, Y., et al. Study on Screening and Evaluation of Foam Drainage Agents for Gas Wells with High Temperature and High Pressure. ACS Omega, 2023.